

Measurement of $^{232}\text{Th}(\text{n},2\text{n})^{231}\text{Th}$ reaction cross-sections at neutron energies of 14.1 MeV and 14.8 MeV using neutron activation method*

LAN Chang-Lin (兰长林),^{1,†} XIE Bao-Lin (解保林),¹ ZHANG Kai (张凯),²
PENG Meng (彭猛),¹ and FANG Kai-Hong (方开洪)¹

¹*School of Nuclear Science and Technology, Lanzhou University, Lanzhou 730000, China*

²*Department of Nuclear Physics, China Institute of Atomic Energy, Beijing 102413, China*

(Received July 31, 2015; accepted in revised form September 18, 2015; published online December 20, 2015)

In this study, the activation cross-sections were measured for $^{232}\text{Th}(\text{n},2\text{n})^{231}\text{Th}$ reactions at neutron energies of 14.1 and 14.8 MeV, which were produced by a neutron generator through a $\text{T}(\text{d},\text{n})^4\text{He}$ reaction. Induced gamma-ray activities were measured using a low background gamma ray spectrometer equipped with a high resolution HPGe detector. In the cross-section calculations, corrections were made regarding the effects of gamma-ray attenuation, dead-time, fluctuation of the neutron flux, and low energy neutrons. The measured cross-sections were compared with the literature data, evaluation data (ENDF-B/VII.1, JENDL-4.0 and CENDL-3.1), and the results of the model calculation (TALYS1.6).

Keywords: $^{232}\text{Th}(\text{n},2\text{n})^{231}\text{Th}$ reaction, Cross-section, Neutron activation method

DOI: [10.13538/j.1001-8042/nst.26.060501](https://doi.org/10.13538/j.1001-8042/nst.26.060501)

I. INTRODUCTION

Accurate knowledge of neutron induced reaction cross-sections around 14 MeV is very useful for the design of fusion reactors, molten salt reactors, hybrid subcritical systems, accelerator driven subcritical systems (ADSs), nuclear transmutations, and additionally for checking and improving nuclear and/or nuclear reaction models. Since thorium added MOX fueled subcritical hybrid reactors are intended for energy production, the cross-section of the $\text{Th}(\text{n},2\text{n})$ reaction plays a key role in the Th-U nuclear fuel cycle [1], especially for the neutron balance calculation due to the relatively high $(\text{n},2\text{n})$ reaction cross-section. In view of its importance, the cross-section of the $^{232}\text{Th}(\text{n},2\text{n})^{231}\text{Th}$ reaction has been measured by a few laboratories, but there is relatively large disagreement and uncertainty among these data. Meanwhile, the discrepancies between the evaluated data files (ENDF/B-VII.1, JEFF-3.2, JENDL-4.0, CENDL-3.1) can reach 30–50% in the energy range of 13 and 15 MeV. Moreover, the above reaction cross-section is currently required within an accuracy of 1–2% in order to be used safely in simulated techniques for predicting the dynamical behavior of complex arrangements in thorium molten salt reactors (TMSR) [2]. Hence, it is necessary to make further precise and accurate measurements to strengthen the reliability of the databases.

In the present work, the cross-sections of the $^{232}\text{Th}(\text{n},2\text{n})^{231}\text{Th}$ reaction were measured in neutron energies of 14.1 and 14.8 MeV using the activation technique. The measured results are discussed and compared with experimental data found in the literature. The results were calculated by a computer code, TALYS 1.6, as well as the evaluated values of the databases.

II. EXPERIMENTAL PROCEDURES

The experiment was carried out using the CPNG-600 neutron generator at China Institute of Atomic Energy (CIAE). Neutrons with a yield of about $\sim 1.5 \times 10^{10} \text{ n}/4\pi\text{s}$ were produced by the $\text{T}(\text{d},\text{n})^4\text{He}$ reaction. The ion beam current was up to 300 μA with an effective deuteron energy of 300 keV. A solid tritium-titanium (T-Ti) target was used in the generator with a thickness of $1.0 \text{ mg}/\text{cm}^2$. During irradiation, the variation of the neutron yield was monitored by accompanying α -particles so that corrections could be made for the fluctuation of the neutron flux. The schematic view of the accompanying α -particle monitor was the same as shown in Ref. [3]. The Au-Si surface barrier detector used in the 135° accompanying α -particle tube was at a distance of 110 cm from the target.

The thorium dioxide powder of 99.7% purity (from China North Nuclear Fuel Corporation Limited) was pressed into circular thin samples with a diameter of 20 mm, and two such ThO_2 targets with a thickness of 1.05 mm and 1.07 mm were used. Each thorium target was placed between two natural aluminum foils of the same diameter. All the Al foils had purities better than 99.99% and a thickness of 0.06 mm. The samples were placed at 0° and 90° angles relative to the deuteron beam direction and centered about the T-Ti target at a distance of about 3.5 cm. The neutron energies in these positions were calculated by the Q equation [4] and compared with the method of cross-section ratios for the $^{90}\text{Zr}(\text{n},2\text{n})^{89\text{m}+\text{g}}\text{Zr}$ and $^{93}\text{Nb}(\text{n},2\text{n})^{92\text{m}}\text{Nb}$ reactions [5, 6] before irradiation. The determined neutron energy was (14.1 ± 0.2) MeV and (14.8 ± 0.2) MeV, respectively.

The radioactivity of each activated product was determined via low background γ -ray spectroscopy by using a coaxial GMX60 HPGe detector (ORTEC, made in USA) with a relative efficiency of 68% and an energy resolution of 1.82 keV FWHM at 1.33 MeV. The distance between the sample and the detector is 5 cm. The efficiency calibration was determined by using point-like calibrated gamma-ray sources. The decay characteristics of the product radioisotopes and the nat-

* Supported by National Natural Science Foundation of China (No. 11205076)

† Corresponding author, lanchl@lzu.edu.cn

TABLE 1. Reactions and associated decay data of activation products

Reaction	Abundance of target isotope η (%)	Q -value (MeV)	Half-life of product $T_{1/2}$	Gamma-ray energy E_γ (keV)	Gamma-ray intensity I_γ (%)
$^{232}\text{Th}(n,2n)^{231}\text{Th}$	100	-6.440	25.52 h	84.2	6.6
$^{27}\text{Al}(n,\alpha)^{24}\text{Na}$	100	-3.132	14.951 h	1368.63	100

TABLE 2. Summary of the cross sections

Reaction	Cross-sections (in mb) at various neutron energies (in MeV)	
	$E_n = (14.1 \pm 0.2) \text{ MeV}$	$E_n = (14.8 \pm 0.2) \text{ MeV}$
$^{232}\text{Th}(n,2n)^{231}\text{Th}$	1342.703 ± 127.56	993.402 ± 95.367
$^{27}\text{Al}(n,\alpha)^{24}\text{Na}$	121.6 ± 0.6	111.9 ± 0.5

ural abundances of the target isotopes under investigation are summarized in Table 1 [7, 8].

The count rates were corrected for contributions from background neutrons, self absorption in the sample, and pile up and coincidence losses of cascade γ -rays. The uncertainties mainly include the counting statistics (1–2%), detection efficiency ($\sim 2\%$), mass of the samples ($< 0.1\%$), neutron energy and fluency uncertainties (2.5%), self-absorption of γ -rays (0.5%), the irradiation, cooling and measuring times ($< 0.8\%$), etc.

III. EXPERIMENT DATA DEDUCTION AND NUCLEAR MODEL CALCULATION

Cross-sections of the $^{27}\text{Al}(n,\alpha)^{24}\text{Na}$ reaction were selected as monitors to measure the cross-section of the $^{232}\text{Th}(n,2n)^{231}\text{Th}$ reaction. The measured cross-sections, σ_x , were calculated by the activation formula [9]:

$$\sigma_x = \frac{[\eta \varepsilon I_\gamma m KSD]_m [\lambda FCA]_x}{[\eta \varepsilon I_\gamma m KSD]_x [\lambda FCA]_m} \sigma_m, \quad (1)$$

$$F = F_s \times F_c \times F_g, \quad (2)$$

$$K = \left[\sum_i^L \Phi_i (1 - e^{-\lambda \Delta t_i}) e^{-\lambda T_i} \right] / \Phi S, \quad (3)$$

where, σ represents the cross-section; η is the abundance of the target nuclide; ε is the full-energy peak efficiency of the measured characteristic γ -ray; I_γ is the γ -ray intensity; m is the mass of sample; K is the neutron fluency fluctuation factor; $S = 1 - e^{-\lambda T}$ is the growth factor of the residual nuclide, λ is the decay constant, and T is the total irradiation time; $D = e^{-\lambda t_1} - e^{-\lambda t_2}$ is the counting collection factor, t_1 and t_2 are time intervals from the end of the irradiation to the start of counting and end of counting, respectively; F is the total correction factor of the activity; C is the measured full-energy peak area, and A is the atomic weight. The footnotes m and x represent the terms of the monitor reaction and the measured reaction, respectively.

In Eq. (2), F_s , F_c , and F_g are the correction factors for the self-absorption of the sample at a given γ -energy and the

coincidence sum effect of cascade γ -rays in the investigated nuclide and in the counting geometry, respectively. And in Eq. (3), we divided the total irradiation time into L parts, where L is the number of time intervals into which the irradiation time is divided, ΔT_i is the duration of the i^{th} time interval, T_i is the time interval from the end of the i^{th} interval to the end of irradiation, Φ_i is the neutron flux averaged over the sample during the ΔT_i , and Φ is the neutron flux averaged over the sample during the total irradiation time T .

The measured $^{232}\text{Th}(n,2n)^{231}\text{Th}$ cross-sections are presented in Table 2 together with the cross-sections of the monitor reaction, $^{27}\text{Al}(n,\alpha)^{24}\text{Na}$ [10].

In this work, the excitation function of the $^{232}\text{Th}(n,2n)^{231}\text{Th}$ reaction cross-sections at different neutron energies from threshold to 20 MeV was calculated theoretically using the computer code TALYS, version 1.6. [11, 12]. The TALYS-1.6 code system is able to analyze and predict nuclear reactions based on physics models and parameterizations. It calculate nuclear reactions involving neutrons, photons, protons, deuterons, tritons, ^3He and α -particles in the 1 keV–200 MeV energy range and for target nuclides with a mass of 12 and heavier. For the ^{232}Th target, the default optical model parameters for neutron values and all possible outgoing channels for a given neutron energy were considered, including inelastic and fission channels [13].

IV. RESULTS AND DISCUSSION

Cross-sections of $^{232}\text{Th}(n,2n)^{231}\text{Th}$ reaction at neutron energies of 14.1 and 14.8 MeV were obtained relative to the $^{27}\text{Al}(n,\alpha)^{24}\text{Na}$ reaction. In the calculations, the cross-sections of the $^{27}\text{Al}(n,\alpha)^{24}\text{Na}$ monitor reaction were obtained by interpolating the evaluated values of the literature. The cross-sections measured in the present work and the cross-sections of the monitor reactions are summarized in Table 2. Our values were measured with approximately 9.5% uncertainty.

Figure 1 shows the cross-section of the $^{232}\text{Th}(n,2n)^{231}\text{Th}$ reaction along with the literature results [14–29]. It can be seen that the experimental $^{232}\text{Th}(n,2n)^{231}\text{Th}$ reaction cross-sections show a sharp increasing trend from threshold to a neutron energy of 8.0 MeV and hereafter remains constant up to a neutron energy of 13.6 MeV. Above a neutron energy of

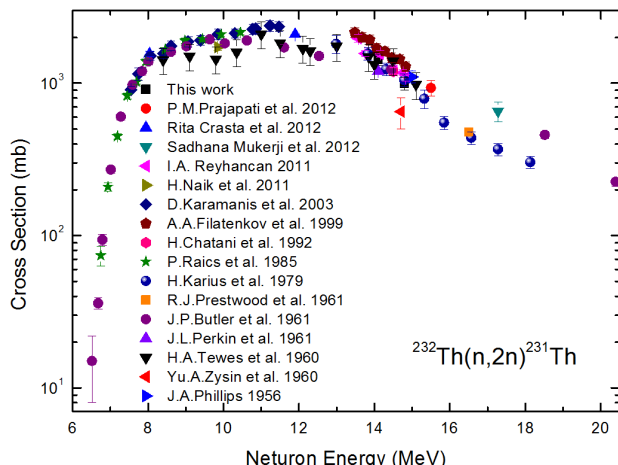


Fig. 1. (Color online) Plot of the experimental $^{232}\text{Th}(\text{n},2\text{n})^{231}\text{Th}$ reaction cross sections as a function of the neutron energy from 6 MeV to 20 MeV.

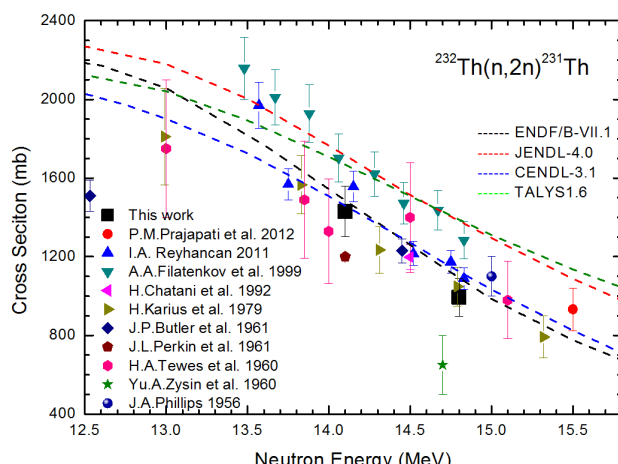


Fig. 2. (Color online) Cross-sections of the $^{232}\text{Th}(\text{n},2\text{n})^{231}\text{Th}$ reaction in the 12.5–15.8 MeV energy range compared to the previous measurements, models calculations (TALYS1.6) and evaluated data from ENDF/B-VII.1, JENDL-4.0, CENDL-3.1.

13.6 MeV the cross-sections show a decreasing trend, mainly due to the opening of the (n,3n) and (n,2nf) reaction channels.

According to the D-T neutron generator, the experimental cross-section measurements were performed between 13–15 MeV neutron energies. In view of this, the measured cross-sections of the $^{232}\text{Th}(\text{n},2\text{n})^{231}\text{Th}$ reaction from the present work and the literature given in EXFOR [30] were plotted in Fig. 2 for the energy range of 12.5–15.8 MeV, along with the evaluated data [31–33], as well as the theoretical values from TALYS1.6. Around the 14 MeV neutron energy range, the present results agreed well with those given by Reyhancan *et al.* [17], Karius *et al.* [23], and Butler *et al.* [25], within experimental uncertainties. From Fig. 2, the ENDF-B/VII.1 and CENDL-3.1 evaluation data files agreed well with our values, but the TALYS1.6 calculated results over predicted the experimental $^{232}\text{Th}(\text{n},2\text{n})^{231}\text{Th}$ reaction cross-section, except the data from Filatenkov *et al.* [20].

V. CONCLUSION

In this work, the activation cross-sections of the $^{232}\text{Th}(\text{n},2\text{n})^{231}\text{Th}$ reaction were obtained in the neutron energies of 14.1 MeV and 14.8 MeV. A considerable improvement in accuracy was achieved. In general, our measurements agreed with recent literature data, but some discrepancies were observed among the literature values, which might be attributed to variations in measurement methods of the neutron flux and/or the samples and nuclear parameters used. The results were compared with previously reported measured cross-sections and TALYS-1.6 nuclear model calculations. The new results measured in this work are useful for verifying the accuracy of the nuclear models used in the calculation of cross-sections and practical applications.

ACKNOWLEDGMENTS

We would like to thank the Intense Neutron Generator group at China Institute of Atomic Energy for performing the irradiations.

[1] Pronyaev V G. Summary Report of the Consultants' Meeting on Assessment of Nuclear Data Needs for Thorium and Other Advanced Cycles, Rep. INDC(NDS)-408, IAEA, Vienna, 1999.

[2] Jiang M H, Xu H J and Dai Z M. Advanced fission energy program-TMSR nuclear energy system. Bulletin of Chinese Academy of Sciences, 2012, **27**: 366–374. (in Chinese) DOI: [10.3969/j.issn.1000-3045.2012.03.016](https://doi.org/10.3969/j.issn.1000-3045.2012.03.016)

[3] Luo J H, Xu X S, Cao X X, *et al.* Activation cross sections and isomeric cross section ratios for the (n,2n) reactions on ^{175}Lu , ^{198}Pt and ^{82}Se from 13.5 to 14.6 MeV. Nucl Instrum Meth B, 2007, **265**: 453–460. DOI: [10.1016/j.nimb.2007.10.005](https://doi.org/10.1016/j.nimb.2007.10.005)

[4] Curtis L F. Introduction to neutron physics. D. Van Nostrand Company, Princeton, NJ, 1969.

[5] Lewis V E and Zieba K J. A transfer standard for $d + t$ neutron fluence and energy. Nucl Instrum Methods, 1980, **179**: 141–144. DOI: [10.1016/0029-554X\(80\)90422-X](https://doi.org/10.1016/0029-554X(80)90422-X)

[6] Luo J H, Du L and Zhao J. A method to determine fast neutron energies in large sample. Nucl Instrum Meth B, 2013, **298**: 61–65. DOI: [10.1016/j.nimb.2013.01.029](https://doi.org/10.1016/j.nimb.2013.01.029)

[7] Browne E and Tuli J K. Nuclear Data Sheets for $A=231$. Nucl Data Sheets, 2013, **114**: 751–840. DOI: [10.1016/j.nds.2013.05.002](https://doi.org/10.1016/j.nds.2013.05.002)

[8] Firestone R B. Nuclear data sheets for $A=24$. Nucl Data Sheets, 2007, **108**: 2319–2392. DOI: [10.1016/j.nds.2007.10.001](https://doi.org/10.1016/j.nds.2007.10.001)

[9] Kong X Z, Wang R, Wang Y C, *et al.* Cross sections for 13.5–14.7 MeV neutron induced reactions on palladium

isotopes. *Appl Radiat Isotopes*, 1999, **50**: 361–364. DOI: [10.1016/S0969-8043\(97\)10144-0](https://doi.org/10.1016/S0969-8043(97)10144-0)

[10] Wagner M, Vonach H, Pavlik A *et al.* Physik daten-physics data, evaluation of cross sections for 14 important neutron-dosimetry reactions, Fachinformationszentrum Karlsruhe, Gesellschaft für wissenschaftlich-technische Information mbH, in the Federal Republic of Germany, No.13-5, 1990.

[11] Koning A, Hilaire S and Gorilev S. TALYS-1.6, A nuclear reaction program. NL-1755 ZG Petten, The Netherlands, 2013. <http://www.talys.eu>

[12] Koning A J and Rochman D. Modern nuclear data evaluation with the TALYS code system. *Nucl Data Sheets*, 2012, **113**: 2841–2934. DOI: [10.1016/j.nds.2012.11.002](https://doi.org/10.1016/j.nds.2012.11.002)

[13] Koning A J and Delaroche J P. Local and global nucleon optical models from 1 keV to 200 MeV. *Nucl Phys A*, 2003, **713**: 231–310. DOI: [10.1016/S0375-9474\(02\)01321-0](https://doi.org/10.1016/S0375-9474(02)01321-0)

[14] Prajapati P M, Naik H, Suryanarayana S V, *et al.* Measurement of the neutron capture cross-sections of ^{232}Th at 5.9 MeV and 15.5 MeV. *Eur Phys J A*, 2012, **48**: 35. DOI: [10.1140/epja/i2012-12035-4](https://doi.org/10.1140/epja/i2012-12035-4)

[15] Rita C, Naik H, Suryanarayana S V, *et al.* Measurement of the $^{232}\text{Th}(\text{n},\gamma)^{233}\text{Th}$ and $^{232}\text{Th}(\text{n},2\text{n})^{231}\text{Th}$ reaction cross-sections at neutron energies of 8.04 ± 0.30 and (11.90 ± 0.35) MeV. *Ann Nucl Energy*, 2012, **47**: 160–165. DOI: [10.1016/j.anucene.2012.02.010](https://doi.org/10.1016/j.anucene.2012.02.010)

[16] Mukerji S, Naik H, Suryanarayana S V, *et al.* Measurement of $^{232}\text{Th}(\text{n},\gamma)$ and $^{232}\text{Th}(\text{n},2\text{n})$ cross-sections at neutron energies of 13.5, 15.5 and 17.28 MeV using neutron activation techniques. *Pramana*, 2012, **79**: 249–262. DOI: [10.1007/s12043-012-0299-0](https://doi.org/10.1007/s12043-012-0299-0)

[17] Reyhanian I A. Measurements and model calculations of activation cross sections for $^{232}\text{Th}(\text{n},2\text{n})^{231}\text{Th}$ reaction between 13.57 and 14.83 MeV neutrons. *Ann Nucl Energy*, 2011, **38**: 2359–2362. DOI: [10.1016/j.anucene.2011.07.032](https://doi.org/10.1016/j.anucene.2011.07.032)

[18] Naik H, Prajapati P M, Suryanarayana S V, *et al.* Measurement of the neutron capture cross-section of ^{232}Th using the neutron activation technique. *Eur Phys J A*, 2011, **47**: 51. DOI: [10.1140/epja/i2011-11051-2](https://doi.org/10.1140/epja/i2011-11051-2)

[19] Karamanis D, Andriamonje S, Assimakopoulos P A, *et al.* Neutron cross-section measurements in the Th-U cycle by the activation method. *Nucl Instrum Meth A*, 2003, **505**: 381–384. DOI: [10.1016/S0168-9002\(03\)01102-1](https://doi.org/10.1016/S0168-9002(03)01102-1)

[20] Filatenkov A A, Chuvaev S V, Aksenov V N, *et al.* Systematic measurement of activation cross sections at neutron energies from 13.4 to 14.9 MeV. Khlopin Radiev Inst, Leningrad Re-

ports No.252, 1999.

[21] Chatani H and Kimura I. Measurement of the $^{232}\text{Th}(\text{n},2\text{n})^{231}\text{Th}$ reaction cross section with 14.5 MeV neutrons. *Ann Nucl Energy*, 1992, **19**: 425–429. DOI: [10.1016/0306-4549\(92\)90065-J](https://doi.org/10.1016/0306-4549(92)90065-J)

[22] Raics P, Daróczy S, Csikai J, *et al.* Measurement of the cross sections for the $^{232}\text{Th}(\text{n},2\text{n})^{231}\text{Th}$ reaction in the 6.745 to 10.450 MeV energy range. *Phys Rev C*, 1985, **32**: 87–91. DOI: [10.1103/PhysRevC.32.87](https://doi.org/10.1103/PhysRevC.32.87)

[23] Karius H, Ackermann A and Scobel W. The pre-equilibrium contribution to the $(\text{n},2\text{n})$ reactions of ^{232}Th and ^{238}U . *J Phys G Nucl Phys*, 1979, **5**: 5. DOI: [10.1088/0305-4616/5/5/011](https://doi.org/10.1088/0305-4616/5/5/011)

[24] Prestwood R J and Bayhurst B P. $(\text{n},2\text{n})$ Excitation functions of several nuclei from 12.0 to 19.8 MeV. *Phys Rev*, 1961, **121**: 1438–1441. DOI: [10.1103/PhysRev.121.1438](https://doi.org/10.1103/PhysRev.121.1438)

[25] Butler J P and Santry D C. The $^{232}\text{Th}(\text{n},2\text{n})^{231}\text{Th}$ cross section from threshold to 20.4 MeV. *Can J Chemistry*, 1961, **39**: 689–696. DOI: [10.1139/v61-083](https://doi.org/10.1139/v61-083)

[26] Perkin J L and Coleman R F. Cross-sections for the $(\text{n},2\text{n})$ reactions of ^{232}Th , ^{238}U and ^{237}Np with 14 MeV neutrons. *J Nucl Energy AB*, 1961, **14**: 69–75. DOI: [10.1016/0368-3230\(61\)90094-5](https://doi.org/10.1016/0368-3230(61)90094-5)

[27] Tewes H A, Caretto A A, Miller A E, *et al.* Excitation functions of neutron-induced reactions. Nuclear and radiation chemical symposium, Chalk River, Ontario, Canada, UCRL-6028-T, CONF-600901-1, Sep.6, 1960.

[28] Zysin Y A, Kovrizhnykh A A, Lbov A A, *et al.* The cross section of the $^{232}\text{Th}(\text{n},2\text{n})^{231}\text{Th}$ at 14.7 MeV. *J Nucl Energy AB*, 1962, **16**: 121. DOI: [10.1016/0368-3230\(62\)90271-9](https://doi.org/10.1016/0368-3230(62)90271-9)

[29] Phillips J A. The $(\text{n},2\text{n})$ cross-section of ^{232}Th for fission neutrons. *J Nucl Energy*, 1958, **7**: 215–219. DOI: [10.1016/0891-3919\(58\)90076-7](https://doi.org/10.1016/0891-3919(58)90076-7)

[30] IAEA-EXFOR Database. <http://www-nds.eaea.org/exfor>

[31] Chadwick M B, Herman M, Obložinský P, *et al.* ENDF/B-VII.1 Nuclear data for science and technology: Cross sections, covariance, fission product yields and decay data. *Nucl Data Sheets*, 2011, **112**: 2887–2996. DOI: [10.1016/j.nds.2011.11.002](https://doi.org/10.1016/j.nds.2011.11.002)

[32] Shibata K, Iwamoto O, Nakagawa T *et al.* JENDL-4.0: a new library for nuclear science and engineering. *J Nucl Sci Technol*, 2011, **48**: 1–30. DOI: [10.1080/18811248.2011.9711675](https://doi.org/10.1080/18811248.2011.9711675)

[33] Zhuang Y X and Shen Q B. CENDL-3: Evaluated Nuclear Data File (ENDF). Database Version of December 22, 2011. <http://www.nndc.bnl.gov/exfor/servlet/E4sSearch2>